Acoustic two-port simulation model for the particle oxidation catalyst (POC®)

Antti HYNNINEN[1]; Mats ÅBOM[2]

[1] VTT Technical Research Centre of Finland

[2] KTH-CCGEx, The Marcus Wallenberg Laboratory, Sweden

ABSTRACT

The reduction of the exhaust noise from internal combustion engine (IC-engine) is mainly managed by proper silencer design, while less attention is paid to the acoustic performance of the after treatment devices (ATD). It is known from the earlier studies, that the transmission loss of a typical ATD unit can be quite significant. An ATD unit for diesel engines is classically assembled from several specific parts such as selective catalytic reducers (SCR), diesel oxidation catalysts (DOC) and diesel particulate filters (DPF). One new alternative to the conventional DPF is the particle oxidation catalyst (POC®). The substrate used in the POC-X type filter consists of fine, corrugated metallic wire mesh screens piled askew and rolled into a cylindrical shape. In this paper an acoustic two-port simulation model for POC-X is sought starting from the classical Kirchhoff solution for prediction of the acoustic wave attenuation in narrow channels. According to experimental studies, correction factors to the narrow channel two-port model are proposed.

Keywords: Two-port, Particle oxidation catalyst   I-INCE Classification of Subjects Number(s): 37.6, 76.9

1. INTRODUCTION

The acoustic two-port simulations of ATD can be found in literature. The acoustic performance of SCR, DOC, and DPF were investigated by Elnady et al. [1], for example. They validated the acoustic 1D models developed by Allam and Åbom presented, e.g. in [2, 3] using measurements and implemented the two-port models to SIDLAB® software [4]. Conventional DPF requires regular active regeneration and periodical ash removal to operate. Alternative after treatment solutions have been developed to avoid these costly maintenance procedures. One of these is the POC-X [5, 6, 7, 8].

The structure of the POC-X substrate forms tortuous channels running through the filter allowing the exhaust gas to either flow through the substrate cells formed from the metallic wire mesh screens or along the tortuous channels in the case of overloaded or blocked substrate (see Fig. 1).

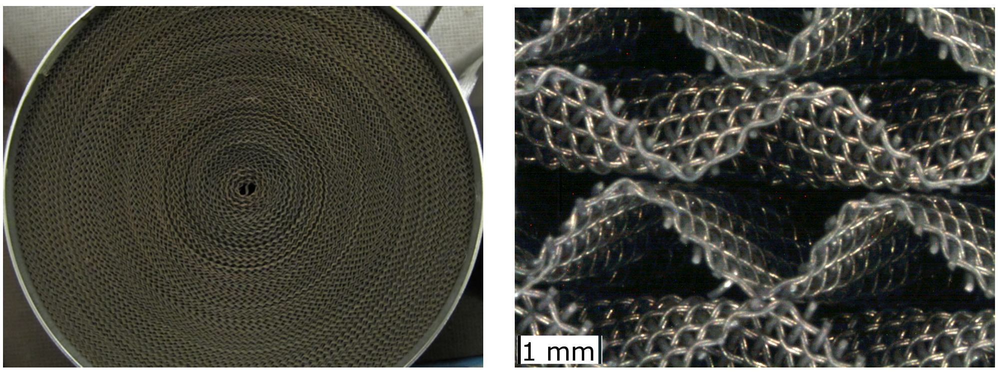

Figure 1 – POC-X type filter (left) and microscope photograph of the substrate cells formed from the metallic wire mesh screens (right).

[1] antti.hynninen@vtt.fi
[2] matsabom@kth.se

The first investigation on the acoustic behaviour of the POC-X was published by Hynninen et al. [9]. In their paper, they presented a frequency independent, plane wave frequency range acoustic two-port simulation model for POC-X based on the pressure drop measurements.

In this paper an acoustic two-port simulation model for POC-X is sought starting from the classical, frequency dependent, Kirchhoff solution for prediction of the acoustic wave attenuation in narrow channels. The simulation model is adjusted with optimized correction factors. Using experimental test data as the reference, the aim is to introduce a two-port model which is valid not only in the plane wave frequency range but also in the higher frequency range with non-plane waves.

2. ACOUSTIC TWO-PORTS

Assuming a linear sound field, the transfer matrix formulation can be used to describe the frequency domain relationship between the acoustic states at the inlet and outlet of the two-port as

$$\left\{ \begin{array}{c} \hat{p}_{in} \\ \hat{q}_{in} \end{array} \right\} = \left[\begin{array}{cc} T_{11} & T_{12} \\ T_{21} & T_{22} \end{array} \right] \left\{ \begin{array}{c} \hat{p}_{out} \\ \hat{q}_{out} \end{array} \right\}, \tag{1}$$

where $\hat{p}$ and $\hat{q}$ are the fourier transforms of the plane wave acoustic pressure and volume velocity at the inlet and outlet as denoted with subscripts *in* and *out*, respectively. The elements T_{xy} of the transfer matrix $\mathbf{T}$ describe the sound reflections and transmissions of the passive system. Using the transfer matrix formalism, the M passive elements can be assembled easily by multiplying the corresponding transfer matrices $\mathbf{T}_m$

$$\mathbf{T}_{tot} = \prod_{m=1}^{M} \mathbf{T}_m. \tag{2}$$

When the total transfer matrix of the system is known, the transmission loss (TL) over the assembled system can be obtained straight forwardly using the transfer matrix elements as presented by Munjal [10]

$$TL = 10log_{10} \left\{ \frac{1}{4} \frac{Z_{out}}{Z_{in}} \left| T_{11} + \frac{T_{12}}{Z_{out}} + T_{21} Z_{in} + T_{22} \frac{Z_{in}}{Z_{out}} \right|^2 \right\}, \tag{3}$$

where Z is the characteristic impedance.

3. WAVE ATTENUATION IN NARROW CHANNELS

In the analytical solution presented, e.g. by Pierce [11] the wave attenuation in a channel can be described using the complex speed of sound c_c and the complex density ρ_c. According to classical Kirchhoff solution [12, 13] these can be calculated as

$$c_c = c_0 \frac{\sqrt{1 - F(s)}}{\sqrt{1 + (\gamma - 1) F(\sigma s)}} \tag{4}$$

and

$$\rho_c = \frac{\rho_0}{1 - F(s)}, \tag{5}$$

where $\gamma = C_p/C_v$ is the ratio of the specific heat coefficient for constant pressure and constant volume, $\sigma^2 = \mu C_p/\kappa$ is the Prandtl number, μ is the shear viscosity coefficient, κ is the gas thermal conductivity constant and

$$F(s) = \frac{2}{s\sqrt{-i}} \frac{J_1(s\sqrt{-i})}{J_0(s\sqrt{-i})}, \tag{6}$$

where $s = r_c\sqrt{\rho_0 \omega/\mu}$ is the Stokes number, r_c is the radius of the channel, ω is the angular frequency, J_0 and J_1 are the zero and first order Bessel functions respectively. Eqns. (4) and (5) are valid for circular channels. If the channel cross-sections is not circular, the radius r_c can be derived from the corresponding hydraulic diameter $r_c = D_{hyd}/2$. Using the complex density and speed of sound, the transfer matrix of a distributed catalyst element is written as

$$\mathbf{T}^{cat} = \left[\begin{array}{cc} cos(k_{cat}L_{cat}) & iZ_{cat}sin(k_{cat}L_{cat}) \\ i/Z_{cat}sin(k_{cat}L_{cat}) & cos(k_{cat}L_{cat}) \end{array} \right], \tag{7}$$

where Z_{cat} is the characteristic impedance of the catalyst element, k_{cat} is the wave number and L_{cat} is the catalyst length. The characteristic impedance of the catalyst element is calculated by dividing the complex speed of sound and density, Eqns. (4) and (5), with the equivalent channel area of the catalyst

$$Z_{cat} = \frac{\rho_c c_c}{R_o S}, \tag{8}$$

where R_o is the open area ratio of the catalyst and S is the total frontal area. The catalyst wave number is $k_{cat} = \omega / c_c$. The channel length depends on the length of the element L and on the skew angle of the corrugations of the sheets α

$$L_{channel} = \frac{L}{cos(\alpha)}. \tag{9}$$

For the uniform and unconnected channels as used in open foil coated (OFC)-type catalysts [9], the catalyst length in Eqn. (7) equals the channel length, i.e. $L_{cat} = L_{channel}$.

In the POC-X type filter, the wire mesh screens forms tortuous channels which are connected to each other. By introducing the POC-X wire mesh filter length correction factor ξ the equivalent channel length can be defined

$$L_{eqv} = \xi L_{channel}. \tag{10}$$

In this paper, the length correction factor ξ is sought using experimental test data as the reference. Using $L_{cat} = L_{eqv}$ in Eqn. (7), the frequency dependent, two-port model for POC-X type filter is defined.

4. FINDING THE CORRECTION FACTORS

In this paper, the correction factors are determined with unconstrained optimization and MATLAB® optimization tool-box. The target is to find the minimum of the objective function starting at an initial estimate. The problem is specified as

$$\min_{\xi} |f(\xi)|, \tag{11}$$

where $f(\xi)$ returns a scalar value for the correction factor ξ. Only plane waves are propagating in the duct up to the cut-on frequency of the first non-plane wave mode. That is $f_{10,cut-on}$, where subscript 10 denotes the number of radial and circumferential nodal lines, respectively. In the plane wave frequency range the simulation results can be compared with the transmission loss determined from the classical two-port measurements. The most common way to describe the acoustic performance of a filter in the high frequency range with non-plane waves is the insertion loss (IL). Therefore the simulation results are compared to the insertion loss after the first non-plane wave mode cut-on frequency.

The target value is defined as the average difference over the samples and as the average difference in the 1/3 octave bands corresponding the plane wave or the non-plane wave frequency range. The piecewise objective function is then

$$f(\xi) = \begin{cases} \frac{1}{M}\sum_m \left(\frac{1}{N}\sum_n \left(\langle TL(\xi) \rangle_{1/3}^{calculated} - \langle TL \rangle_{1/3}^{measured} \right)_n \right)_m & ,f < f_{10,cut-on} \\ \\ \frac{1}{M}\sum_m \left(\frac{1}{N}\sum_n \left(\langle TL(\xi) \rangle_{1/3}^{calculated} - \langle IL \rangle_{1/3}^{measured} \right)_n \right)_m & ,f \geq f_{10,cut-on}, \end{cases} \tag{12}$$

where $\langle \, \rangle_{1/3}$ denotes summing in 1/3 octave bands, N is the number of samples and M is the number of 1/3 octave frequency bands in the corresponding plane wave and non-plane wave frequency ranges. The results of the optimization are the best fit wire mesh filter length correction factors.

5. TEST DATA

The procedure was applied to experimental data determined to four POC-X type filters [9]. Data of the tested filters is presented in Table 1. Diameter of the tested filters is $\varnothing$= 200 mm. Transmission loss of the filters was determined from the measured two-port data in the 1/3 octave frequency bands from center frequency of 25 Hz to 800 Hz using scattering matrix method [14]. The insertion loss was measured using standardized method [15] up to the 1/3 octave band with center frequency of 8000 Hz.

The transfer matrices of the filters were determined according to section 3 and the transmission loss was determined using Eqn. (3). The gas properties used in the simulations are listed in Table 2.

Table 1 – Data for the tested samples. Cell density unit cpsi means cells per square inch.

cell density (cpsi)	L (mm)	D_{hyd} (mm)	R_o (%)	α (deg)
400	120	1.23	0.69	34
200	120	1.96	0.79	20
300	180	1.51	0.74	34
300	100	1.51	0.74	34

Table 2 – The gas properties used in the two-port simulations.

T (°C)	ρ_0 (kg/m^3)	C_p (kJ/(kg K))	$\mu \times 10^5$ (Pa s)	$\kappa \times 10^2$ (W/(m K))	γ (-)
20	1.19	1.01	1.82	2.58	1.4

6. RESULTS

The correction factors were determined with the MATLAB® optimization tool-box and Eqns. (11) and (12). Number of samples $N = 4$ in Eqn. (12) and the number of 1/3 octave frequency bands $M = 16$ in the plane wave frequency range and $M = 11$ in the non-plane wave frequency range. As the result, the best fit wire mesh filter length correction factors were found

$$\xi = \begin{cases} 1.03 & , f < f_{10,cut-on} \\ 1.48 & , f \geq f_{10,cut-on}. \end{cases} \tag{13}$$

The simulated and measured transmission losses and insertion losses are presented in Figs. 2 and 3, respectively. For comparison, also the uncorrected simulation results ($\xi = 1.00$) are presented.

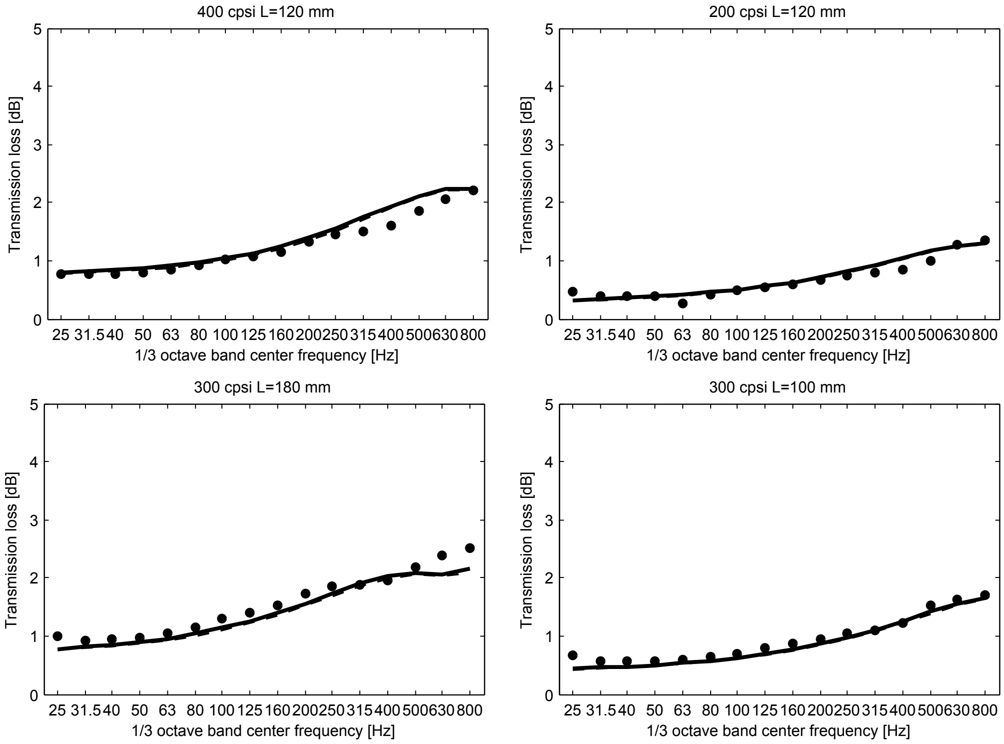

Figure 2 – The simulated (lines) and measured (marks) transmission losses of the tested filters in the plane wave frequency range. The simulation results with the correction factor of $\xi = 1.00$ are plotted with dashed lines and results with the correction factor of $\xi = 1.03$ with solid lines.

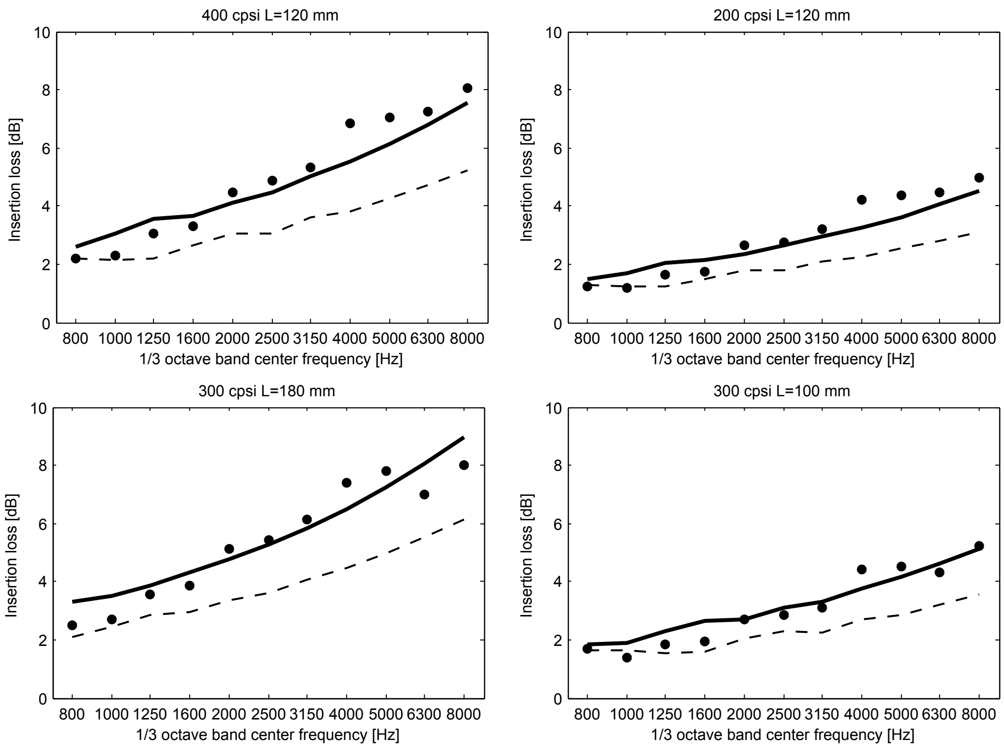

Figure 3 – The simulated (lines) and measured (marks) insertion losses of the tested filters in the non-plane wave frequency range. The simulation results with the correction factor of $\xi = 1.00$ are plotted with dashed lines and results with the correction factor of $\xi = 1.48$ with solid lines.

7. DISCUSSION AND CONCLUSIONS

It can be noted from the upper sub figures in Figs. 2 and 3 that the attenuation increases with the channel density, cpsi. It is also clearly visible in the lower sub figures that the attenuation increases with the filter length, which is intuitively correct.

The best fit correction factor in the plane wave frequency range is 1.03, which means that the filter length used in the classical Kirchhoff solution with uniform channels must be increased by 3%. It can be noted that the dashed and solid lines in Fig. 2 are almost on top of each other. Based on that, the frequency dependent, low frequency, plane wave frequency range acoustic behaviour of POC-X filter can be simulated with reasonable accuracy assuming unconnected, uniform channels, i.e. $\xi = 1.00$.

The corresponding filter length increase in the non-plane wave frequency range is 48% compared to the basic Kirchhoff solution. As can be noted from Fig. 3, the simulated results with the correction factor of $\xi = 1.48$ fits with the measurements quite good. The deviation in the investigated high frequency range is approximately within 1 dB. Compared to the uncorrected results plotted with dashed lines the improvement is significant.

It should be noted that instead of fitting each simulation model to the corresponding measurement data, the best fitting equivalent filter length was determined in the plane wave and non-plane wave frequency range for the set of samples. Data fitting based on experiments is necessary when the detailed data of the filter construction, i.e. wire mesh geometry, porosity parameters, etc. does not appear to be readily available.

Using the approach presented in this paper, the classical plane wave frequency range Kirchhoff solution for prediction of the acoustic wave attenuation in narrow channels is extended to the non-plane wave frequency range in the case of POC-X type filter. Using the computationally effective two-port model for POC-X type filter is especially useful when optimizing the complete exhaust system of an IC-engine for the maximum noise reduction.

More work is necessary to address the non-plane frequency range phenomena behind the 48 % increase in the equivalent length as well as the effect of the mean flow on the attenuation, which was beyond this study. For these purposes a more detailed simulation model of the POC-X filter must be used.

REFERENCES

1. T. Elnady, S. Elsaadany and D. Herrin, "Investigation of the acoustic performance of after treatment devices", *SAE Int. J. of Pass. Cars - Mech. Sys.*, **4**(2), 1068–1075, (2011).
2. S. Allam and M. Åbom, "Modeling and testing of after-treatment devices", *J. Vib. Acoust.*, **128**(3), 347–356, (2006).
3. S. Allam and M. Åbom, "Acoustic modelling and testing of diesel particulate filters", *J. Sound Vibr.*, **288**(1), 255–273, (2005).
4. T. Elnady and M. Åbom, "SIDLAB: new 1D sound propagation simulation software for complex duct networks", *International Congress on Sound and Vibration*, (2006).
5. K. Lehtoranta, P. Matilainen, J. Åsenbrygg, A. Lievonen, T. Kinnunen, J. Keskinen, and A. Solla, "Particle oxidation catalyst in light duty and heavy duty diesel applications", *SAE Technical Paper 2007-24-0093*, (2007).
6. K. Lehtoranta, P. Matilainen, T. Kinnunen, J. Heikkilä, T. Rönkkö, J. Keskinen, and T. Murtonen, "Diesel particle emission reduction by a particle oxidation catalyst", *SAE Technical Paper 2009-01-2705*, (2009).
7. T. Kinnunen, P. Matilainen, D. Scheder, W. Czika, D. Waters, and G. Russ, "Particle oxidation catalyst (POC®)-from diesel to gdi-studies on particulate number and mass efficiency", *SAE Technical Paper 2012-01-0845*, (2012).
8. M. Happonen, P. Matilainen, K. Kanniainen, T. Kinnunen, P. Karjalainen, J. Heikkilä, T. Rönkkö, J. Keskinen, T. Lähde, A. Malinen, L. Pirjola, and T. Tzamkiozis, "The effect of a particle oxidation catalyst (POC®) on particle emissions of a GDI car during transient engine operation", *SAE Technical Paper 2013-01-0839*, (2013).
9. A. Hynninen, H. Isomoisio, M. Åbom, and E. Nousiainen, "On acoustic performance of the particle oxidation catalyst POC®", *Baltic Nordic Acoustic Meeting - BNAM*, (2014).
10. M. L. Munjal, *Acoustics of Ducts and Mufflers with Application to Exhaust and Ventilation System Design*, John Wiley & Sons, New York, (1987).

11. A. Pierce, *Acoustics: an introduction to its physical principles and applications*, Acoustical Society of America, (1989).

12. C. Zwikker and C. Kosten, *Sound absorption materials*, (1949).

13. D. Keefe, "Acoustical wave propagation in cylindrical ducts: Transmission line parameter approximations for isothermal and nonisothermal boundary conditions", *J. Acoust. Soc. Am.*, **75**(1), 58–62, (1984).

14. M. Åbom, "Measurement of the scattering-matrix of acoustical two-ports", *Mech. Sys. Signal Proc.*, **5**(2), 89–104, (1991).

15. *Acoustics - laboratory measurement procedures for ducted silencers and air-terminal units - insertion loss, flow noise and total pressure loss*, International Standard ISO-7235, International Organization for Standardization, Geneva, Switzerland, (2003).